Collision rates estimated from exact N -body simulations of a one-dimensional plasma

Etienne Gravier, Thomas Drouot, Maxime Lesur, Alejandro Guillevic, Guillaume Lo-Cascio, Jérôme Moritz, Dominique Escande, Giovanni Manfredi

Collision rates estimated from exact N-body simulations of a one-dimensional plasma

Etienne Gravier,* Thomas Drouot, Maxime Lesur, Alejandro Guillevic, Guillaume Lo-Cascio, and Jérôme Moritz

Université de Lorraine, CNRS, Institut Jean Lamour, UMR 7198, F-54000 Nancy, France

Dominique Escande

Aix-Marseille Université, CNRS, PIIM, UMR 7345, F-13000 Marseille, France

Giovanni Manfredi†

Université de Strasbourg, CNRS, Institut de Physique et Chimie des Matériaux de Strasbourg, UMR 7504, F-67000 Strasbourg, France

(Dated: November 16, 2022)

Abstract

In a plasma, the charged particles interact via long-range forces and this interaction causes the plasma to exhibit collective effects. If the graininess or coupling parameter g goes to zero (ideal collisionless plasma), two-body collisions are negligible while collective effects dominate the dynamics. In contrast, when $g \approx 1$ collisions play a significant role. To study the transition between a collisionless and a collisional regime, a N-body code was developed and used in this work. The code solves exactly, in one spatial dimension, the dynamics of N infinite parallel plane sheets for both ion and electron populations. We illustrate the transition between individual and collective effects by studying two basic plasma phenomena, the two-stream instability and Langmuir waves, for different values of g. The numerical collision rates given by the N-body code increase linearly with g for both phenomena, although with proportionality factors that differ by roughly a factor of two, a discrepancy that may be accounted for by the different initial conditions. All in all, the usual collision rates published in the literature (Spitzer collisionality) appear to compare rather well with the rates observed in our simulations.

*Electronic address: etienne.gravier@univ-lorraine.fr

†Electronic address: giovanni.manfredi@ipcms.unistra.fr

I. INTRODUCTION

The most accurate way to simulate the many-body plasma dynamics is by solving the full N-body system of Newton's equations. But for a typical fusion or astrophysical plasmas, it is obviously impossible to follow the trajectories of each one of the $\approx 10^{23}$ particles that constitute the plasma. Hence the need for kinetic models, which are mean-field models that neglect microscopic two-body collisions and only retain the macroscopic self-consistent electromagnetic fields. Kinetic models typically solve the evolution equation (Vlasov equation) of a one-particle probability distribution in the six-dimensional phase space, coupled to the Maxwell equations for the fields.

Rigourously, kinetic models can be derived from the full N-body dynamics through a BBGKY hierarchy truncated to the lowest order, which amounts to neglecting two-body and higher-order correlations between the particles. The smallness parameter that defines this hierarchy and justifies the truncation procedure is the so-called coupling or "graininess" parameter g, which is proportional to the ratio of the kinetic energy to the Coulomb energy. Ideal collisionless plasmas are characterized by $g \ll 1$, while strongly coupled plasmas have $g \geq 1$.

Even though fusion plasmas are not collision-dominated, a collision operator is often needed for simulating the plasma behavior on long timescales, for instance to take into account neoclassical transport in tokamaks, which can be dominant when a transport barrier is triggered, or to model the diffusion of high-Z impurities [1, 2]. For this purpose, the relevant Vlasov equations are augmented by a collision term, often in the form of a simple Bhatnagar-Gross-Krook (BGK) operator [3]. The collision rate involved in this collision operator is then given by some Spitzer-like formula [4].

However, this simple procedure is conceptually shaky. The Vlasov equation is already an averaged equation, and the electromagnetic fields that appear there are mean macroscopic fields. Hence, adding to this Vlasov equation a collision term based on the microscopic collision frequency may lead to an incorrect estimation of the effects of the collisions. Recent works [4–6], based on a weak-turbulence calculation starting from the Klimontovich equation and including all wave numbers, suggest a modification of the collision operator. Using this theory, it was estimated that the collisional damping of Langmuir waves is up to two orders of magnitude smaller than the one predicted by a BGK operator [4]. In other works [7, 8] the authors solve either a Vlasov-like equation with ad-hoc collision terms (eq. 1 in [7]) or a Fokker-Planck equation (eq. 6 in [8]).

The present work aims at investigating a simple one-dimensional (1D) N-body model, in order to extract the exact collision rates and compare them to those given by the heuristic Spitzer formula. We want to stress that our approach is based on the N-body Newton equations for the charged

particles. Therefore, we have here a microscopic model that includes, at least potentially, all plasma effects, both collective (such as Landau damping) and individual (such as collisional damping). We will focus on two typical plasma phenomena, namely plasma Langmuir waves and the two-stream instability. As our N-body model is 1D, whereas collision rates are usually estimated in 3D, the comparison can only be approximate, and should be regarded as a first step aimed at clarifying the predictions put forward in Refs. [4, 5].

In the past, several computer experiments were performed with 1D N-body models, investigating various phenomena such as Debye shielding and plasma oscillations [9, 10]. The relaxation towards a Maxwellian distribution was also studied, revealing different scalings of the relaxation time for sub-populations of the particles and for the overall population [11]. The relaxation times were compared to the results of the Lenard-Balescu equation [12]. Other works investigated similar relaxation problems for the dynamics of self-gravitating systems [13].

The present paper is organized as follows. The N-body model and corresponding computational code are described in Sec. II. In Sec. III, we study the impact of collisions on the two-stream instability and estimate the collision frequency by subtracting the observed N-body instability rate from the theoretical collisionless instability rate. In Sec. IV, a similar analysis is performed for Langmuir waves. Comparison with a Vlasov kinetic code allowed us to study the coexistence of collisional damping and Landau damping. Finally, in Sec. V we summarize the preceding results and discuss the dependence of the collision rates on the plasma coupling parameter g. Conclusions are drawn in Sec. VI.

II. ONE-DIMENSIONAL N-BODY MODEL AND COMPUTATIONAL CODE

We consider a two-component plasma made of N electron sheets and N ion sheets with surface charge density $\pm\sigma$. The plasma is confined between two reflecting walls, separated by a distance L, where L is the length of the box (see Fig. 1, top panel). There is no magnetic field. We consider infinite sheets in the direction perpendicular to the x axis, hence the electric field between the sheets is constant, and is equal to an integer multiple of $\sigma/2\epsilon_0$. Thus, the total electric field has a step-like profile and the motion of the sheet is uniformly accelerated as long as it does not cross one of its neighbors (Fig. 1, bottom panel). As the electric field is constant between two planes and using Newton's law, the equation of motion can be integrated exactly up to computer round-off errors.

In the remainder of the paper, lengths are normalized to the Debye length λ_{De}, times are

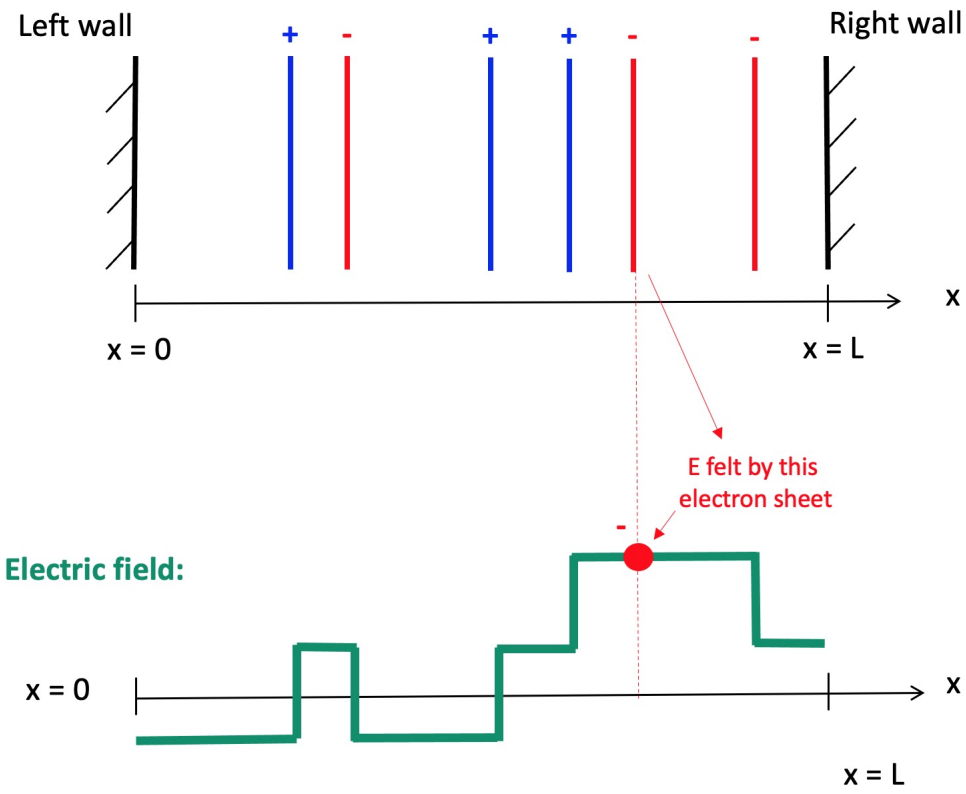

FIG. 1: Schematic view of the 1D planar geometry of the simulations. Top panel: System of N electron and N ion planar sheets, confined between two walls separated by a distance L. Bottom panel: The total electric field has a step-like profile.

normalized to ω_{pe}^{-1}, and velocities to the electron thermal velocity v_{Te}. Starting from Newton's second law applied to one sheet labeled j, the normalized acceleration $\hat{a}_j$ that the sheet experiences is:

$$\hat{a}_j = \frac{\hat{L}}{2N} c_j \frac{m_e}{m_j} [2Q_{g_j} + c_j], \tag{1}$$

where $\hat{L}$ is the length of the box normalized to the Debye length, $2N$ is the total number of sheets (ions and electrons), m_e is the mass of one electron, m_j is the mass of one particle that belongs to the sheet j (ion or electron), Q_{g_j} is the number of sheets located on the left side of the considered sheet j. The sign of the charge belonging to sheet j is c_j, and is equal to $c_j = +1$ for ion sheets and $c_j = -1$ for electron sheets.

As $\hat{a}_j$ is constant between two sheets, we can evolve the dynamical variables v_j and x_j of a single sheet by integrating the equations of motion, which can be done analytically in between two successive collisions, as long as the j-th sheet does not cross one of its two neighbors. After a crossing, the sheets experience a new constant field. Then the trajectories of the sheets in

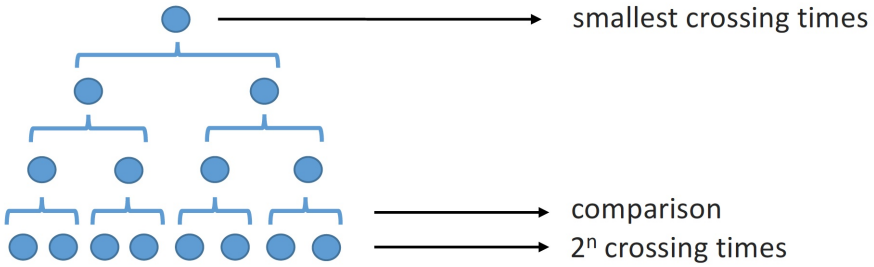

FIG. 2: Heap based algorithm, following [14]: Starting from the $2^n = 2N$ crossing times at the bottom of the heap, the crossing times are compared by pairs and the smallest one ends up at the top of the heap.

phase space are known without any approximation except for the round-off errors due to the finite number of digits to code real numbers the computer. We have checked that the total energy remains constant, with a relative error close to 10^{-13}. In this code, the sheets pass freely through one another, interacting only via their coupling to the electric field, and, as particles interact via long-range forces, two-body collisions as well as collective effects are both taken into account by the model. We also consider that the sheets collide elastically with the walls so that they reverse their velocities whenever they hit one of the walls.

The algorithm starts by computing the collision time of each sheet with its neighbor to the right, or with the wall. Then the smallest crossing time is identified, and the system is evolved up to just before this event. Actually only the two crossing sheets are evolved, while the others are frozen. The time when a sheet last experienced a crossing is recorded in a table. Finally the replacement on the index numbers j and $j+1$ of the two sheets is performed.

The most time consuming operation in the code is the search of the minimum collision time. In order to minimize this step, the collision times are ordered on a heap [14]. The crossing times in the heap obey the following heap condition: each element in a child node is greater than or equal to the elements in its parent node. The smallest time is located at the top of the heap (Fig. 2).

It is not necessary to update all the states of particles while processing the heap. For a large number of sheets, i.e. a large value of N, the operation count is dominated by the cost of reordering the heap after each crossing, which goes asymptotically as $\log N$ [14]. We introduce an indexing array, mapping the position in the heap to the position of the sheets in space. Therefore, this algorithm determines the smallest crossing time at a low numerical cost, but also maps the crossing times in the heap to the spatial positions of the sheets. In the end, the overall duration of a typical run scales as $N \log N$.

III. TWO-STREAM INSTABILITY

As a first example, we consider the case of two cold oppositely-directed electron streams with velocities $\pm v_0$, and heavy ions ($m_i \gg m_e$) with zero velocity. The ions will hardly move on the electronic time scales relevant to this study, and only act as a homogeneous neutralizing background. A random generator is used to distribute the positions of the sheets at $t = 0$. This two-stream configuration can then be unstable under certain conditions. The growth rate of the instability may be derived from the linearized Vlasov-Poisson equations for the electrons:

$$\frac{\partial f_e}{\partial t} + v_x \frac{\partial f_e}{\partial x} - \frac{eE}{m_e} \frac{\partial f_e}{\partial v_x} = 0, \tag{2}$$

$$\frac{\partial E}{\partial x} = \frac{e}{\varepsilon_0} \left(n_0 - \int_{-\infty}^{+\infty} f_e dv_x \right), \tag{3}$$

with n_0 the ion density, here assumed to be constant and equal to the electron plasma density at equilibrium, $e = +1.6 \times 10^{-19}$ C, $m_e = 9.1 \times 10^{-31}$ kg, E the electric field, ε_0 is the dielectric constant in vacuum. The initial electron distribution function is taken as $f_e(x, v_x, t = 0) = f_0(v) = \frac{1}{2} n_0 [\delta(v_x - v_0) + \delta(v_x + v_0)]$, where δ denotes the Dirac delta function, i.e. the streams are assumed to be cold. Linearizing the Vlasov-Poisson equations and expanding in plane waves $\sim e^{i(kx - \omega t)}$, we obtain the instability growth rate γ as the imaginary part of the frequency ω:

$$\gamma = \sqrt{\frac{-2k^2 v_0^2 - \omega_{pe}^2 + \omega_{pe}^2 \sqrt{1 + \frac{8k^2 v_0^2}{\omega_{pe}^2}}}{2}}, \tag{4}$$

where k is the wave number and ω_{pe} is the electron plasma frequency.

As the beams are initially cold, their thermal velocity is zero. However, for long times ($t \to \infty$) the electron population will eventually relax to an equilibrium Maxwellian distribution with thermal velocity v_{Te}. At thermal equilibrium, all the initial drift kinetic energy of the streams ($\frac{1}{2} m_e v_0^2$) will be converted into thermal energy ($k_B T_e = \frac{1}{2} m_e v_{Te}^2$, where k_B is the Boltzmann constant and v_{Te} the electron thermal speed), so that $v_{Te} = v_0$. The effective Debye length is then defined as $\lambda_{De} = v_{Te}/\omega_{pe}$.

From Eq. (4), the maximum linear growth rate of the instability is $\gamma_{max} = 0.3536\ \omega_{pe}$, with $k_{max} \lambda_{De} = 0.6124$. The initial perturbation is provided by the intrinsic numerical noise. The length of the box is chosen to be $L = 10.2606\, \lambda_{De}$, so that the first mode is the most unstable one, i.e., $k_{max} = 2\pi/L$. Hereafter this linear collisionless growth rate will be denoted $\gamma_{no-coll} = \gamma_{max}$,

and will be compared to the instability growth rate obtained from the N-body code, denoted γ_{NB}. As the total potential energy of the two-stream system is expected to increase exponentially with time ($\exp(2\gamma_{NB}t)$) during the linear phase of the instability, γ_{NB} can be easily extracted from the calculated data.

In Fig. 3, $2\gamma_{NB}$ is plotted as a function of N. The horizontal line corresponds to the expected value when collisions are neglected ($2\gamma_{NB} = 2\gamma_{no-coll} = 0.7071$). For values of N smaller than 2000, the linear growth rate of the two-stream instability is smaller than the one expected without collisions. The instability is slowed down by collisions, as expected [15].

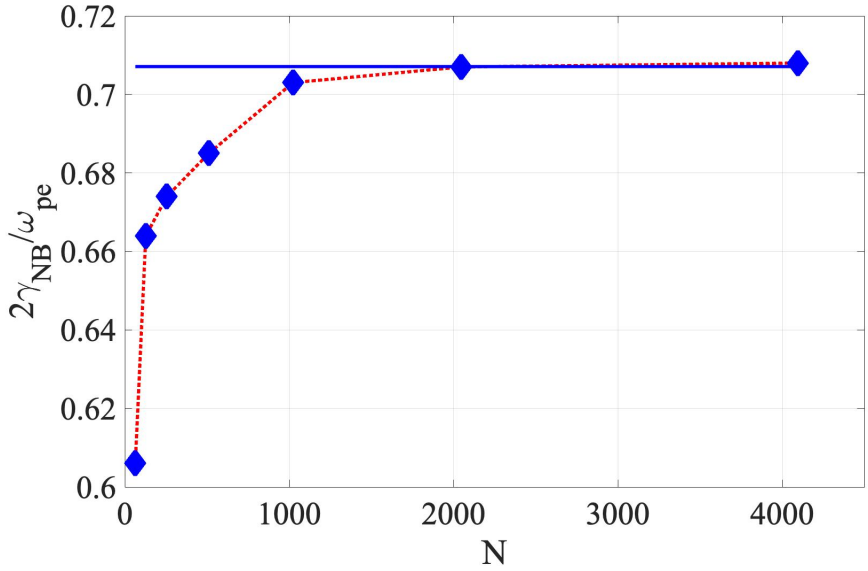

FIG. 3: Measured linear instability growth rate $2\gamma_{NB}$ plotted against the number of sheets N. The horizontal blue line corresponds to the expected value when collisions are neglected.

Here, our working hypothesis is that the growth and damping rates are additive. Therefore, the collision rate due to two-body Coulomb collisions, denoted $\gamma_{coll_{NB}}$, can be written as the difference between the theoretical collisionless growth rate ($\gamma_{no-coll}$) and the observed numerical growth rate of the instability (γ_{NB}):

$$\gamma_{coll_{NB}} = \gamma_{no-coll} - \gamma_{NB}. \tag{5}$$

The dependence of $\gamma_{coll_{NB}}$ on N is shown in Fig. 4.

The hypothesis of Eq. (5) is in agreement with the linear theory of the Vlasov equation augmented by a BGK collision operator $(\partial f_e/\partial t)_{coll} = -\nu(f_e - f_M)$, where ν is the BGK collision rate and f_M is the Maxwellian distribution [15], which predicts that the effective linear growth rate

is lowered by the collision rate. This property was also verified by numerical simulations of the Vlasov-BGK equation using a semi-lagrangian Vlasov code [15, 16].

The importance of collective versus individual two-body effects can be measured using the so-called graininess or coupling parameter g, which for our 1D model reads as [17]:

$$g = \frac{1}{n\lambda_{De}} = \frac{1}{\frac{N}{L}\lambda_{De}} = \frac{\hat{L}}{N}, \tag{6}$$

where $n = N/L$ is the plasma density and $\hat{L} = L/\lambda_{De}$ is the normalized length of the computational box ($\hat{L} \approx 10$ in the present case). When the graininess parameter is of order unity or larger, the plasma is dominated by individual effects, i.e. two-body collisions. Again, we observe that the two-body collisions can be neglected when N is larger than 1000 ($g \lesssim 10^{-2}$).

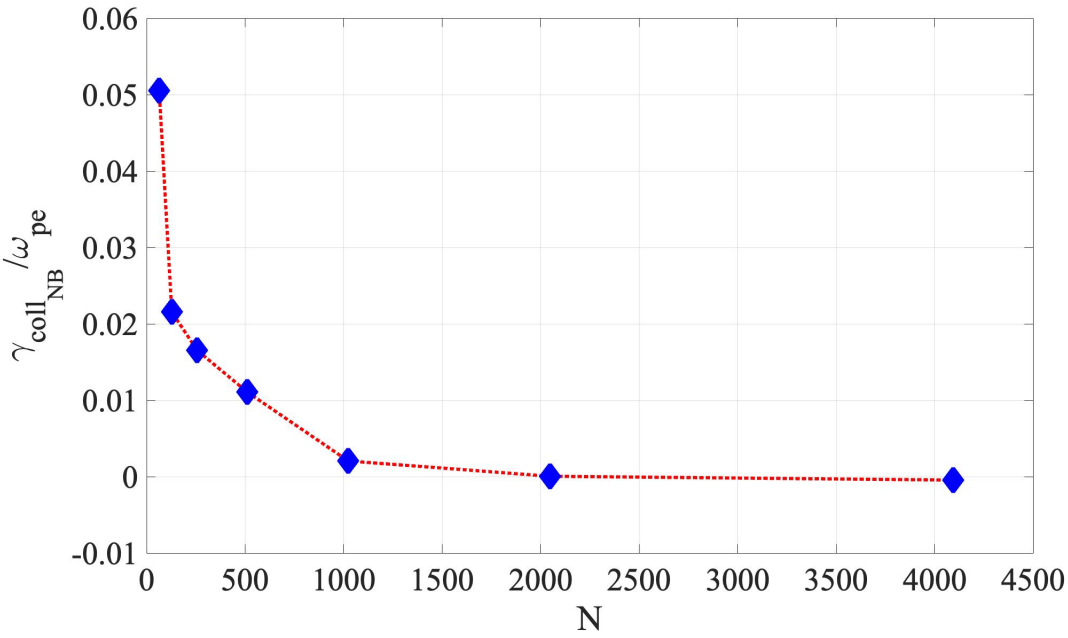

FIG. 4: Collision rate $\gamma_{coll_{NB}}$ obtained from the N-body code for the two-stream instability, as a function of the number of sheets N.

Finally, it should be mentioned that, on longer timescales, the two streams are destroyed by the instability and the system evolves towards thermal equilibrium. This occurs over a characteristic time that scales as $g^{-2} \sim (n\lambda_{De})^2$, in agreement with earlier results [9, 11, 12].

IV. LANGMUIR WAVES

We now consider the phenomenon of plasma oscillations and Langmuir waves. If we shift the electrons with respect to the positive ions, the mutual attraction of the two species acts as a restoring force that causes the electrons to oscillate relative to the ions at a certain frequency ω. The well-known Bohm-Gross dispersion relation [18] quantifies this effect:

$$\omega^2 = \omega_{pe}^2 + 3k^2 v_{Te}^2 \tag{7}$$

If the wave number k is equal to zero (homogeneous perturbation), the electrons should oscillate at the plasma frequency. We shall first consider this case.

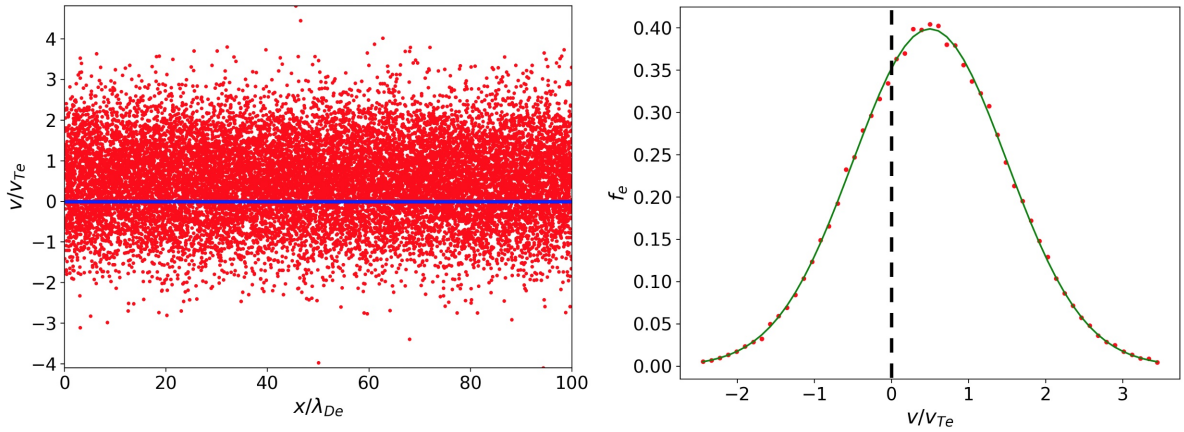

FIG. 5: Electron (red) and ion (blue) phase-space distribution function (left panel) and electron velocity distribution (right panel) for $v_{kick} = 0.5\, v_{Te}$.

At $t = 0$, the distribution of the electrons is a Maxwellian. In order to excite the plasma oscillations, we adopt the same procedure as described in [10]: we impart to all the electrons a positive velocity kick, meaning that each v_j is instantaneously changed to $v_j + v_{kick}$. This procedure is equivalent to applying a large and almost instantaneous electric field to the electrons between $t = 0$ and $t = \tau$, which induces a velocity change $eE\tau/m_e = v_{kick}$, with $E \to \infty$, $\tau \to 0$, but $E\tau$ finite (Fig. 5).

In order to assess the plasma oscillations, we study the evolution of $\bar{v}_e(t)$, the spatial average of the electron velocities. Indeed $\bar{v}_e(t)$ is much less sensitive to thermal fluctuations than the density or the electric potential. As a first check, we measured the oscillation period for different values of N and different lengths L of the box. As expected, we found a period equal to $2\pi/\omega_{pe}$ with a relative discrepancy less than 5%.

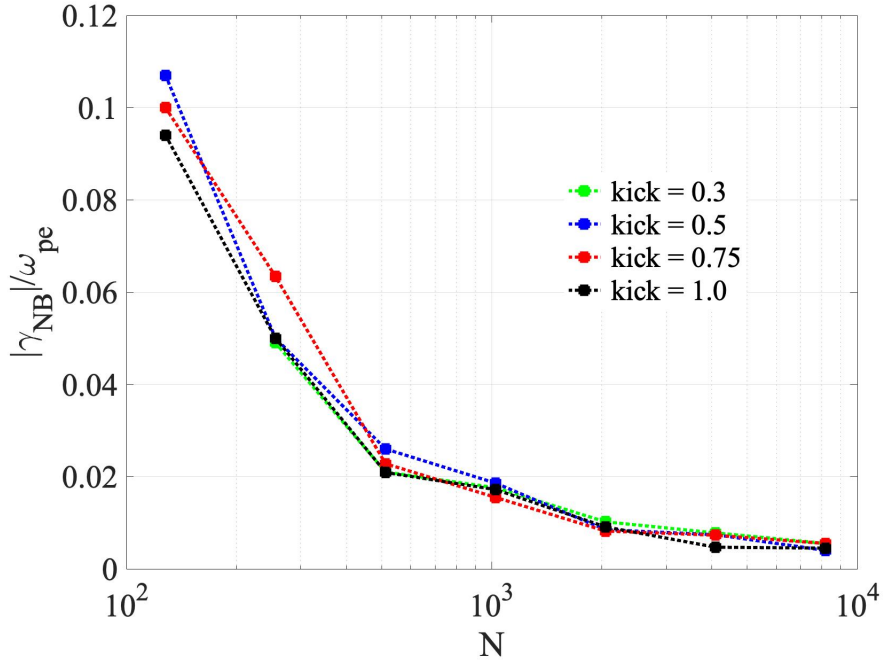

FIG. 6: Measured collision rate γ_{NB} plotted against the number of sheets N, in the case of plasma oscillations, for four different values of the kick (0.3, 0.5, 0.75 and 1.0 v_{Te}). In this case $\gamma_{NB} = \gamma_{coll_{NB}}$ because the mode $k = 0$ is considered (plasma oscillations with no Landau damping).

Next, we estimate the damping rate by plotting the amplitude of the oscillations on a semi-logarithmic scale and determine its slope using a least squares method. As in this case there is neither instability nor Landau damping ($k = 0$), the observed damping rate directly represents the collision rate $\gamma_{coll_{NB}}$. The results are presented in Fig. 6. The collision rate is plotted for four values of the kick ranging from 0.3 v_{Te} to 1.0 v_{Te}, with $L = 100\,\lambda_{De}$. We observe that the collision rates depend little on the initial kick. Again, as observed in the case of the two-stream instability, collisional damping becomes significant for values of N below $N \approx 2000$ ($g > 5 \times 10^{-2}$).

Finally, in order to investigate the influence of collisions on the total damping of Langmuir waves, we consider modes with $k \neq 0$. In order to excite a particular wave number, we modulate the initial velocity of each particle as follows:

$$v_j = v_{j,Maxwell} + v_0 \sin\left(m\frac{2\pi}{L}x_j\right) \tag{8}$$

where $v_{j,Maxwell}$ is the velocity of the sheet j, located at $x = x_j$, before the kick, and m is the mode number. The wave number k is then equal to $2\pi m/L$. The amplitude v_0 is chosen to be $0.1\,v_{Te}$.

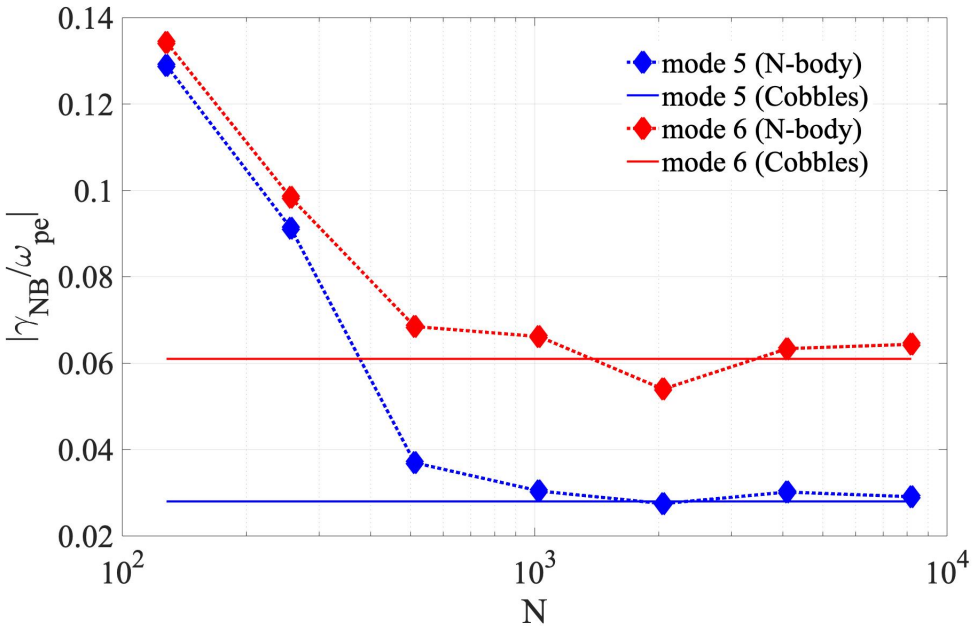

FIG. 7: Measured damping rates γ_{NB} plotted against the number of sheets N, for Langmuir waves. The horizontal lines correspond to the Landau damping rates given by the Vlasov code COBBLES [16] and PIC code [19]. We have $\gamma_{NB} = \gamma_{coll_{NB}} + \gamma_{Landau}$. For large values of N, the collision rate becomes negligible.

The measured damping rates are shown in Fig. 7 for modes $m = 5$ and $m = 6$. The simulations were repeated several times, more than five hundred times for the smaller values of N, in order to reduce statistical errors by ensemble averaging. In the case of Langmuir waves with $k \neq 0$, Landau damping can compete with collisional damping. To investigate this competition between Landau and collisional damping, a Vlasov code (COBBLES [16]) and a Particle-In-Cell (PIC) code [19], without any collision operators, were used to determine the Landau damping rates for the $m = 5$ and $m = 6$ modes. Both codes yield $\gamma_{Landau} = 0.028$ for $m = 5$ and $\gamma_{Landau} = 0.061$ for $m = 6$, with the same initial conditions as those used in the N-body code. In Fig. 7, the horizontal lines correspond to the Landau damping rates given by the Vlasov and PIC codes.

Again, for small values of g ($g < 5 \times 10^{-2}$), i. e. large values of the number of sheets ($N > 2000$), the effect of Coulomb collisions can be neglected when compared to the Landau damping rate. For both modes $m = 5$ and $m = 6$ the transition is located at the same values of N (and therefore of g).

V. TWO-BODY COLLISION RATES

In the preceding sections, we found that – in all three cases considered here of plasma waves ($k = 0$), Langmuir waves ($k \neq 0$), and two-stream instability – collisional effects start playing a role for $g \gtrsim 10^{-2}$. The agreement of the three results suggests the method we used to determine the two-body collision rate can be trusted to deduce some general laws.

Fig. 8 summarizes the findings detailed in the preceding sections, augmented by some further simulations performed with different parameters, such as different stream velocities or box lengths. The red and blue lines represent linear regression fits of the collision rates with the coupling parameter, $\gamma_{coll_{NB}} \propto g$, with slopes equal to 0.326 (coefficient of determination, $R^2 = 0.97$) for the two-stream instability, and 0.135 ($R^2 = 0.98$) for the plasma oscillations. This linear dependence on g appears to be rather natural, as two-body collisions are a first-order effect (in g^1) in a BBGKY hierarchy, where the mean-field Vlasov approximation holds at the lowest order (g^0). We will address shortly the discrepancy between the collision rate observed for the two-stream instability and for plasma waves.

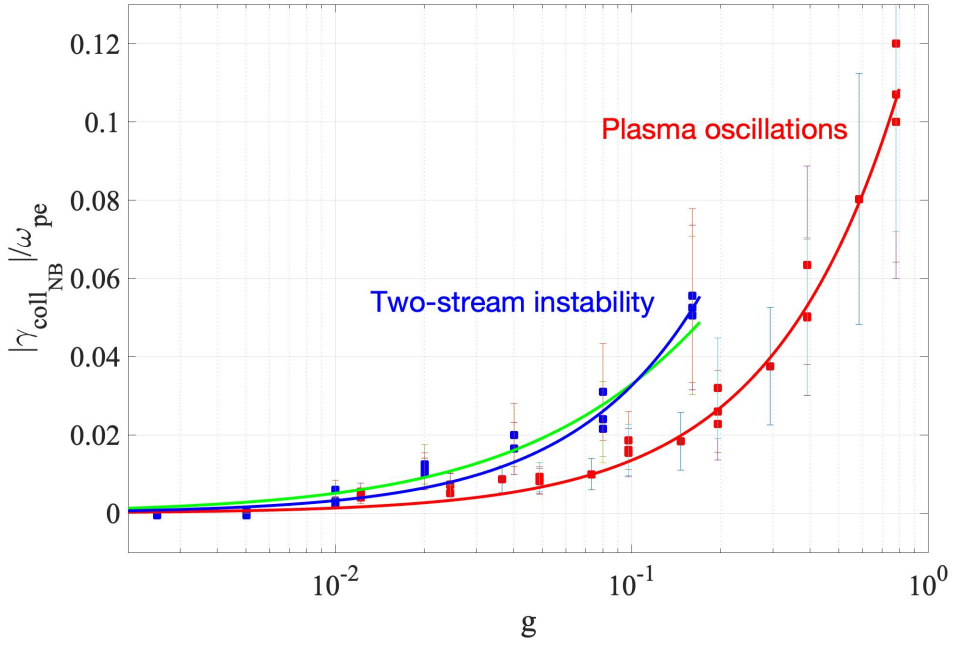

FIG. 8: Measured collision rates $\gamma_{coll_{NB}}$ as a function of the coupling parameter g, in the case of the two-stream instability (blue) and plasma oscillations (in red). The solid lines correspond to the linear fits ($\gamma_{coll_{NB}} \propto g$), with a slope equal to 0.326 for the two-stream instability, and 0.135 for plasma oscillations. The solid green line corresponds to Eq. (10).

The comparison with the standard collision rates published in the literature is not straightforward, because usual estimations are done for realistic 3D plasmas, whereas our model is 1D. Nevertheless we attempt a comparison in order to fix the ideas and check that the 1D results are not too far from reality.

For an electron with a velocity v passing throughout many ions, the electron-ion collision rate is [20, 21]:

$$\nu_{ei_{single}} = \frac{ne^4}{4\pi\epsilon_0^2 m_e^{1/2}(k_B T_e)^{3/2}} \ln\Lambda, \tag{9}$$

where n is the plasma density, $\ln\Lambda = \ln(\lambda_{De}/\lambda_L)$ is the Coulomb logarithm, and λ_L is the smallest impact parameter – i.e., two-body collisions that lead to large deflection angles have been neglected in the calculation. λ_L is equal to $2e^2/(4\pi\epsilon_0 m_e v_{Te}^2)$, and therefore $\ln\Lambda = \ln(2\pi/g)$. Nevertheless, we stress that the notions of impact parameter and Coulomb logarithm have no counterpart for 1D collisions, as approaching particles will always cross each other, and the electric force is constant rather that decreasing as the square of the distance.

Normalizing to the electron plasma frequency yields:

$$\frac{\gamma_{single}}{\omega_{pe}} = \frac{\nu_{ei_{single}}}{\omega_{pe}} = \frac{g}{4\pi} \ln\left(\frac{2\pi}{g}\right). \tag{10}$$

The above collision rate is plotted on Fig. 8 (green line), and reproduces quite well the results for the two-stream instability. This seems rather natural, as Eq. (9) applies to electrons all having the same velocity, which is indeed the case for our monochromatic streams. Nevertheless, it should be noted that the expression of $\nu_{ei_{single}}$ given in Eq. (10) takes into account the Coulomb logarithm and its $g \ln g$ dependence on the coupling parameter g, whereas the blue and red lines in Fig. 8 are simply proportional to g. Although the order of magnitude given by Eq. (10) is in agreement with the collision rates measured from the N-body simulations, we emphasize that the comparison is not straightforward as the Coulomb logarithm has no counterpart for 1D collisions.

For the case of plasma oscillations, the starting distribution function is a Maxwellian. In that case, the electrons with velocities larger than v_{Te} experience fewer collisions with the ions (as ν_{ei} is proportional to $1/v^3$). Hence, the collision rate has to be averaged over the electron distribution function [21], which yields [22]:

$$\langle\nu_{ei}\rangle = \sqrt{\frac{2}{\pi}}\, \nu_{ei_{single}} \approx 0.8\, \nu_{ei_{single}}. \tag{11}$$

A further correction factor to $\langle\nu_{ei}\rangle$ should be included to take into account the distortion of the electronic distribution that appears in the presence of an electric field [21, 23–25]. Electrons of

different velocities respond differently to the combined effect of an electric field and collisions with ions. The faster electrons are less collisional and therefore are more effectively accelerated by the field, which modifies the shape of the distribution function. When all these effects are included, the net result is the Spitzer collisionality, about twice as small as the simple Maxwellian-averaged estimate:

$$\gamma_{Spitzer} \approx 0.5 \, \langle \nu_{ei} \rangle \approx 0.4 \, \nu_{ei_{single}}. \tag{12}$$

The Spitzer rate, which takes into account the Maxwellian distribution and other corrections, should be more relevant to the collisional damping of plasma waves. Indeed, the ratio between the Spitzer and the single-particle collision rates $\gamma_{Spitzer}/\gamma_{single} \approx 0.4$ is similar to the ratio of the observed collision rates for the two-body instability (monochromatic velocity distribution) and for the plasma waves (Maxwellian distribution): $0.135/0.326 = 0.41$ (see Fig. 8).

To test the above ideas, a further series of numerical experiments was performed for plasma oscillations with cold monochromatic electrons. The slope of the damping rate as a function of g was found to be equal to 0.364 ($R^2 = 0.99$), close to the one obtained for the two-stream instability (0.326). Therefore, the same factor ≈ 0.4 is observed between the slope of the damping rate of plasma oscillations for cold monochromatic electrons and the slope of the damping rate of the same plasma oscillations for a Maxwellian distribution. This is a further hint that the different observed slopes are indeed due to the different types of velocity distributions used in the simulations.

To conclude, we underline that the usual 3D collision rates published in the literature, such as Eq. (10), appear to compare rather well with the rates observed in our simulations. Although the substantial difference between 1D and 3D plasmas precludes a definite conclusion from these numerical experiments, these results seem in contradiction with a recent theoretical analysis [4, 5] where both collective and individual effects were incorporated from first principles. Further work will be necessary to elucidate this discrepancy.

VI. CONCLUSION

The purpose of this work was to provide an estimation of the collision rates by performing computer experiments with a 1D N-body plasma model. The advantage of this model is that it contains both collective and collisional effects, and that the relevant equations of motion can be integrated exactly (up to round-off errors). Therefore it provides an ideal tool to compare theoretical estimates with measured collision rates.

We implemented such comparison for three relevant cases involving basic plasma phenomena: the two-stream instability, simple plasma waves at the plasma frequency, and Langmuir waves obeying the Bohm-Gross dispersion relation. When collisional effects were competing with either an instability or with collisionless Landau damping, the collision rate was obtained by simply subtracting the collisionless rate from the observed one.

The collision rates observed in all three cases were of comparable magnitude, pointing at an intrinsic collisional origin, independent on the details of the phenomena at play. The collision rate for the case of plasma oscillations was found to be slightly smaller (by a factor 0.4) compared to the collision rate for the two-stream instability. This discrepancy was explained in terms of the initial conditions used: Maxwellian distribution for the former case and monochromatic beams for the latter. Using the corrective factors provided in the literature, we could justify this small difference.

The observed collision rates were also well approximated by the standard "Spitzer-like" [24, 25] rates usually published in the literature, in contrast to what was suggested by recent theoretical results in 3D [4, 5]. Further work remains to be done to extend the present results to a more realistic 3D scenario.

Acknowledgments

The authors would like to thank Jean-Louis Rouet, Pierre Bertrand, and Xavier Caron for fruitful discussions.

---

[1] T. Fülöp and P. Helander, Phys. Plasmas **6**, 3066 (1999)

[2] P. Donnel, X. Garbet, Y. Sarazin, V. Grandgirard, N. Bouzat, E. Caschera, G. Dif-Pradalier, P. Ghendrih, C. Gillot, G. Latu, C. Passeron, Plasma Phys. Control. Fusion **61**, 044006 (2019)

[3] P. L. Bhatnagar, E. P. Gross, and M. Krook Phys. Rev. **94**, 511 (1954)

[4] S. F. Tigik, L. F. Ziebell and P. H. Yoon, Phys. Plasmas **23**, 064504 (2016)

[5] P.H. Yoon, L.F. Ziebell, E.P. Kontar and R. Schlickeiser, Phys. Rev. E **93**, 033203 (2016)

[6] D. F. Escande, D. Bénisti, Y. Elskens, D. Zarzoso and F. Doveil, Rev. Mod. Plasma Phys. **2**, 9 (2018)

[7] J. W. Banks, S. Brunner, R. L. Berger and T. M. Tran, Phys. Plasmas **23**, 032108 (2016)

[8] S. F. Tigik, L. F. Ziebell, P. H. Yoon and E. P. Kontar, A&A **586**, A19 (2016)

[9] J. Dawson, Phys. Fluids **5**, 445 (1962)

[10] A. D. Boozer, Am. J. Phys. **78**, 6 (2010)

[11] J. L. Rouet and M. R. Feix, Phys. Fluids B **3**, 1830 (1991)

[12] P. Ricci and G. Lapenta, Phys. Plasmas **9**, 430 (2002)

[13] J. L. Rouet and M. R. Feix, Phys. Rev. E **59**, 73 (1999)

[14] A. Noullez, D. Fanelli and E. Aurell, J. Comp. Phys. **186**, 697 (2003)

[15] W. P. Gula and C. K. Chu, Phys. Fluids **16**, 1135 (1973)

[16] M. Lesur, Y. Idomura and X. Garbet, Phys. Plasmas **16**, 092305 (2009)

[17] J. L. Rouet and G. Manfredi, Transport Theory and Statistical Physics **34**, 1-11 (2005)

[18] D. Bohm and E. P. Gross, Phys. Rev. **75**, 1851 (1949)

[19] J. Moritz, E. Faudot, S. Devaux and S. Heuraux, Phys. Plasmas **23**, 062509 (2016)

[20] K. Nishikawa and M. Wakatani, *Plasma Physics* (Springer, Berlin, 1990)

[21] R. J. Goldston and P. H. Rutherford, *Introduction to Plasma Physics* (Institute of Physics Press, Bristol, 1995)

[22] The averaged collision rate given in Ref. [21] differs by a factor 1/3 from the one of Eq. (11). This is due to the fat that Ref. [21] uses a 3D Maxwellian distribution to perform the average, whereas we average over a 1D distribution.

[23] A. Kuritsyn, M. Yamada, S. Gerhardt, H. Ji, R. Kulsrud, Y. Ren, Phys. Plasmas **13**, 055703 (2006)

[24] R. S. Cohen, L. Spitzer, P. McR. Routly, Phys. Rev. **80**, 230 (1950)

[25] L. Spitzer, R. Härm, Phys. Rev. **89**, 977 (1953)